ISSN 0036-0244, Russian Journal of Physical Chemistry A, 2022, Vol. 96, No. 8, pp. 1715–1718. © Pleiades Publishing, Ltd., 2022.
Russian Text © The Author(s), 2022, published in Zhurnal Fizicheskoi Khimii, 2022, Vol. 96, No. 8, pp. 1165–1169.

PHYSICAL CHEMISTRY OF NANOCLUSTERS AND NANOMATERIALS

Studying the Effect of Doping $Au_{20}(SR)_{16}$ Cluster with Copper and Silver in the Activation of CO and O_2, Based on DFT Data

P. S. Bandurist[a,*], D. A. Pichugina[a], and N. E. Kuzmenko[a]

[a] *Faculty of Chemistry, Moscow State University, Moscow, 119991 Russia*

**e-mail: banduristpavel@gmail.com*

Received December 28, 2021; revised December 28, 2021; accepted February 1, 2022

Abstract—Density functional theory (DFT) (PBE) is used to calculate the structure of bimetallic clusters $Cu@Au_{19}(SCH_3)_{16}$ and $Ag@Au_{19}(SCH_3)_{16}$, which are of interest as precursors for obtaining nanoparticles of controlled size. It is shown that silver occupies a position in the core of a cluster, while copper can be found in both the core and its shell. Models of O_2 and CO adsorption on $Cu@Au_{19}(SCH_3)_{16}$ and $Ag@Au_{19}(SCH_3)_{16}$ show that copper in a cluster's shell promotes the activation of CO. In a cluster's core, it has a positive effect on the gold atoms of the staple fragment, enhancing the activation of CO. O_2 can be activated on $Cu(shell)@Au_{19}(SCH_3)_{16}$, making the latter a promising catalytic system for reactions with the participation of O_2 and SO.

Keywords: oxygen, carbon dioxide, copper, silver, density functional theory, synergistic effect

DOI: 10.1134/S0036024422080040

INTRODUCTION

Bimetallic metal nanoparticles are widely used in catalysis, electronics, and nanotechnology [1]. At a certain ratio of metals in a particle, centers appear that have a specific distribution of metals (the ensemble effect) and/or electron density (the charge effect) [2]. The chemical and physical properties of bimetallic nanoparticles can differ considerably from monometallic analogs as a result of such effects, leading to a substantial increase in catalytic activity in particular [3–7]. Heterogeneous catalysts that contain Au–Ag nanoparticles display higher catalytic activity in CO oxidation than monometallic Ag and Au nanoparticles [3, 4]. A similar effect has been observed for bimetallic catalysts that contain Au and Cu [5]. It is well known that Au–Pd nanoparticles can be used effectively in synthesizing H_2O_2 [6, 7].

The development of the synthesis of gold nanoparticles stabilized by thiolate ligands ($Au_n(SR)_m$) has opened up unique opportunities for preparing heterogeneous catalysts characterized by a narrow size distribution of nanoparticles [8, 9] and using them in the oxidation of CO [10, 11]. A structural feature of $Au_n(SR)_m$ is a shell formed by staple fragments $-S(R)-(Au-S(R))_x-$ that blocks the active centers of the catalyst. This has been confirmed via quantum-chemical modeling of the interaction between $Au_{20}(SCH_3)_{16}$ and O_2 and CO, according to which molecules are not activated and the cluster shell is preserved [12]. The cluster can be preliminarily activated and the shell partially removed during thermal annealing at the stage of preparing the heterogeneous catalyst [13], which is likely to cause agglomeration and the loss of a fixed particle size.

An alternative way of changing the properties of $Au_n(SR)_m$ is to introduce another metal into the cluster. There are several examples in the literature of obtaining bimetallic nanoclusters $M_x@Au_{n-x}(SR)_m$ (M = Cu, Ag) [14–17], but questions about their structure, heteroatom position, and catalytic properties remain open. The aim of this work was to calculate the structure of bimetallic clusters $M@Au_{19}(SCH_3)_{16}$ (M = Cu, Ag) and predict their reactivity with respect to CO and O_2 using the Density Functional Theory.

CALCULATION PROCEDURE

The geometries of bimetallic $Cu@Au_{19}(SCH_3)_{16}$ and $Ag@Au_{19}(SCH_3)_{16}$ clusters and complexes of them with O_2 and CO were optimized and their energies were calculated using the Density Functional Theory with the PBE functional [18] with the full-electron scalar-relativistic basis set in [19]. The contribution from zero-point energy was calculated in a harmonic approximation. The calculations were made using the Priroda program [20].

The reactions between bimetallic clusters and O_2 and CO were

$$M@Au_{19}(SCH_3)_{16} + O_2 = O_2\_M@Au_{19}(SCH_3)_{16}, \quad (1)$$

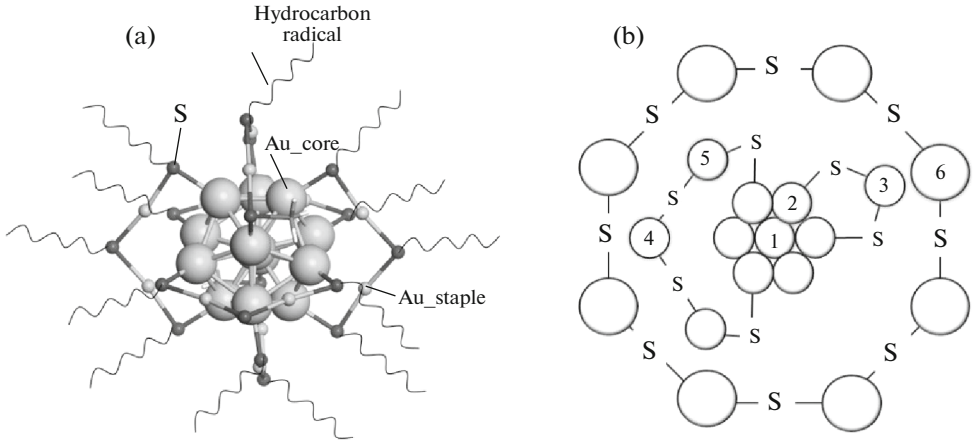

Fig. 1. (a) Structure of a $Au_{20}(SR)_{16}$ cluster and (b) schematic representation of possible positions of copper and silver atoms: (1) central position in the core of the cluster; (2) on the surface of the core; (3) in a monomeric fragment; (4, 5) in different positions of a trimeric fragment; and (6) in the octameric ring.

$$M@Au_{19}(SCH_3)_{16} + CO = CO\_M@Au_{19}(SCH_3)_{16}. \quad (2)$$

The change in energy was calculated from the total energy of all participants in reactions (1) and (2), allowing for the zero-point energy:

$$\Delta E = E(O_2\_M@Au_{19}(SCH_3)_{16}) - E(M@Au_{19}(SCH_3)_{16}) - E(O_2),$$

$$\Delta E = E(CO\_M@Au_{19}(SCH_3)_{16}) - E(M@Au_{19}(SCH_3)_{16}) - E(CO).$$

The energies of complexes $O_2\_M@Au_{19}(SCH_3)_{16}$ were calculated in the singlet and triplet electronic states. The frequencies of oscillation were determined in a harmonic approximation.

RESULTS AND DISCUSSION

At the first stage, we identified non-equivalent positions in $Au_{20}(SCH_3)_{16}$ where copper or silver could be found. According to X-ray diffraction data [21] and quantum-chemical calculations [12], the cluster is formed by a Au_7 core surrounded by $-S(R)-(Au-S(R))_x-$ fragments of different compositions: two monomer fragments ($x = 1$), a trimeric fragment ($x = 3$), and an octameric ring ($x = 8$) (Fig. 1a). We can therefore distinguish six possible positions for a heteroatom: (1) in the center of the core, (2) on the surface of the core, (3) in the monomeric fragment, (4, 5) two different positions in the trimeric fragment, and (6) in the cyclic fragment (Fig. 1b).

Table 1. Relative energies of $M@Au_{19}(SCH_3)_{16}$ isomers (kJ/mol)

Position	Cu	Ag
1	6	0
2	7	1
3	0	13
4	18	25
5	5	12
6	5	9

Six possible $M@Au_{19}(SCH_3)_{16}$ isomers were considered for each heteroatom, and the geometry was optimized with no limits on symmetry. Note that replacing the gold atom with copper or silver atom did not change the overall structure of a cluster (Fig. 1a). Isomer energies calculated relative to the most stable $Cu@Au_{19}(SCH_3)_{16}$ and $Ag@Au_{19}(SCH_3)_{16}$ are presented in Table 1. The structure of the most stable $Cu@Au_{19}(SCH_3)_{16}$ (isomer 3) corresponds to the arrangement of copper in a short monomeric fragment. It should be noted that the energies of isomers 3 and 1, 2, 5, and 6 differ little. We may therefore assume copper can be in the core and occupy positions in all staple groups, except for the position 4. This is consistent with data from works in which a $Cu_xAu_{25-x}(SC_2H_4Ph)_{18}$ ($x = 1-5$) cluster with copper in its core was obtained [14], and $[Au_{13}Cu_2(PPh_3)_6(SPy)_6]^+$, $[Au_{13}Cu_4(PPh_2Py)_4(SC_6H_4\text{-}tert\text{-}C_4H_9)_8]^+$, and $[Au_{13}Cu_8(SPy)_{12}]^+$ were obtained in which copper was a part of their staple fragments [15].

According to the calculations for the structure of $Ag@Au_{19}(SCH_3)_{16}$, the best location for silver is in the core of the cluster (positions 1 and 2). Earlier calculations of the structure of clusters of different compositions $[Au_{25-x}Ag_x(SH)_{18}]^-$ ($x = 1, 2, 4, 6, 8, 10, 12$) [17] also showed the best location for silver is on the surface of the cluster's core.

We modeled the interaction between CO and $M@Au_{19}(SCH_3)_{16}$ (M = Cu, Ag) clusters in which the heteroatom is in the core of the cluster (isomer 1) or in

Table 2. Change in energy during interaction between bimetallic clusters $M@Au_{19}(SCH_3)_{16}$ that differ in the location of M, with O_2 and CO (ΔE, kJ/mol); M–C and M–O equilibrium distances in complexes (Å); and harmonic frequencies of CO and O_2 vibrations in complexes (cm^{-1})

Molecule	Position M	M	ΔE	R(M–C)/R(M–O)	ω(CO)/ω(O_2)
CO	3	Cu	–64	1.82	2051
		Ag	–12	2.68	2059
		Au	–10	2.97	2081
	1	Cu	–21	1.91	2044
		Ag	–10	2.98	2083
		Au	–10	2.97	2081
O_2	3	Cu	–22	2.08	1256
		Ag	–15	2.81	1371
		Au	–12	3.10	1420
	1	Cu	–12	3.08	1412
		Ag	–12	3.11	1414
		Au	–12	3.10	1420

The calculated value of the frequency of oscillation in CO is 2130 cm^{-1}. In O_2, it is 1458 cm^{-1}.

the shell, which is part of the monomeric fragment (isomer 3). Calculated changes in energy during the formation of $CO\_M@Au_{19}(SCH_3)_{16}$ complexes, M–CO distances, and harmonic frequencies of C–O vibrations as a criterion for the activation of a molecule are presented in Table 2, where similar values are also given for a monometallic $Au_{20}(SCH_3)_{16}$ cluster. Considerable activation of CO is observed when copper is in the shell (isomer 3), where the change in energy is –64 kJ/mol. CO bonds to the copper atom at a fairly short Cu–C distance in the complex: 1.82 Å (Fig. 2a). CO bonds more weakly when copper is localized in the core of the cluster. Coordination in the $CO\_Cu(core)@Au_{19}(SCH_3)_{16}$ complex proceeds over the gold atoms in the staple fragment (Fig. 2b) at the considerable Au–C distance of 1.91 Å. The change in energy during the formation of $CO\_Cu(core)@Au_{19}(SCH_3)_{16}$ is much smaller than for $CO\_Cu(shell)@Au_{19}(SCH_3)_{16}$: –21 kJ/mol. Note that copper in the core of a cluster changes the properties of gold atoms in the staple fragment: $Cu(core)Au_{19}(SCH_3)_{16}$ activates CO better than $Au_{20}(SCH_3)_{16}$, as is seen from the lower frequency of C–O vibrations and the shorter Au–C distance in the complex. A synergistic effect was therefore observed for copper in the activation of CO on bimetallic clusters, since copper does not participate directly in the activation of CO. Instead, it affects the gold atoms in the staple fragment on which the CO bonds. Table 2 shows this effect is not typical of $Ag@Au_{19}(SCH_3)_{16}$. With bimetallic clusters $Ag(shell)@Au_{19}(SCH_3)_{16}$ and $Ag(core)@Au_{19}(SCH_3)_{16}$, CO bonds as weakly as on a monometallic $Au_{20}(SCH_3)_{16}$ cluster.

We next modeled the interaction between O_2 and $M@Au_{19}(SCH_3)_{16}$ (M = Cu, Ag) clusters, in which the

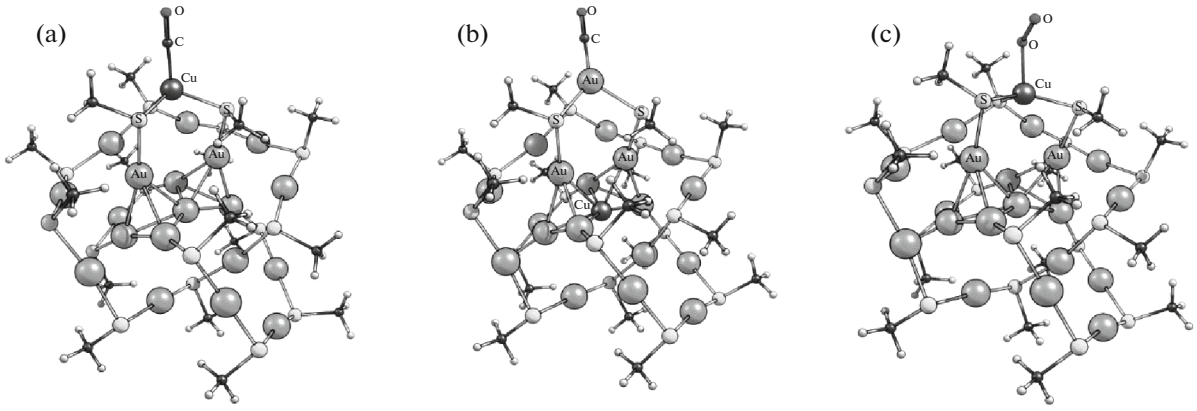

Fig. 2. Optimized structures of $CO\_Cu(shell)@Au_{19}(SCH_3)_{16}$ and $CO\_Cu(core)@Au_{19}(SCH_3)_{16}$.

heteroatom is in the core of the cluster (isomer 1) or in the shell, which is part of the monomeric fragment (isomer 3) (Table 2). If the heteroatom is in the core of the cluster, it has no effect on O_2 bonding, since the change in energy during the formation of complexes with oxygen is −12 for mono- and bimetallic clusters. Better activation of O_2 is observed for a Cu(shell)@$Au_{19}(SCH_3)_{16}$ cluster than one that is monometallic (−22 kJ/mol) (Fig. 2c). Copper in the shell of a cluster therefore promotes the activation of O_2, and thus better CO oxidation.

CONCLUSIONS

The bimetallic Cu@$Au_{19}(SCH_3)_{16}$ system is a promising one for the activation of CO and O_2. When copper is in the cluster's shell, it participates directly in the activation of both CO and O_2, creating a structural effect characteristic of certain bimetallic particles. Copper in Cu(core)@$Au_{19}(SCH_3)_{16}$ and Cu(shell)@$Au_{19}(SCH_3)_{16}$ also has an electronic effect, since the calculated values of the difference in energy between the highest vacant and lowest occupied molecular orbitals of the clusters (172 and 153 kJ/mol) are much lower than for a monometallic cluster (184 kJ/mol). A smaller difference raises the reactivity of the bimetallic cluster.

ACKNOWLEDGMENTS

This work was performed on equipment at the Complex for Modeling and Processing Data of Mega-Class Research Facilities, National Research Center Kurchatov Institute, http://ckp.nrcki.ru/.

REFERENCES

1. K. Loza, M. Heggen, and M. Epple, Adv. Funct. Mater. **30**, 1909260 (2020). https://doi.org/10.1002/adfm.201909260
2. P. Liu and J. K. Nørskov, Phys. Chem. Chem. Phys. **3**, 3814 (2001). https://doi.org/10.1039/B103525H
3. J. Haeck, N. Veldeman, P. Claes, et al., J. Phys. Chem. A **115**, 2103 (2011). https://doi.org/10.1021/jp111257s
4. Y. Kotolevich, E. Pakrieva, E. Kolobova, et al., Catalysts **11**, 799 (2021). https://doi.org/10.3390/catal11070799
5. N. Austin and G. Mpourmpakis, J. Phys. Chem. C **118**, 18521 (2014). https://doi.org/10.1021/jp504015a
6. A. V. Beletskaya, D. A. Pichugina, A. F. Shestakov, et al., J. Phys. Chem. A **117**, 6817 (2013). https://doi.org/10.1021/jp4040437
7. G. Li, J. Edwards, A. F. Carley, et al., Catal. Today **122**, 361 (2007). https://doi.org/10.1016/j.cattod.2007.01.019
8. D. A. Pichugina, N. E. Kuz'menko, and A. F. Shestakov, Russ. Chem. Rev. **84**, 1114 (2015). https://doi.org/10.1070/RCR4493
9. J. Kilmartin, R. Sarip, R. Grau-Crespo, et al., ACS Catal. **2**, 957 (2012). https://doi.org/10.1021/cs2006263
10. B. Kumar, T. Kawawaki, N. Shimizu, et al., Nanoscale **12**, 9969 (2020). https://doi.org/10.1039/D0NR00702A
11. X. Nie, C. Zeng, X. Ma, et al., Nanoscale **5**, 5912 (2013). https://doi.org/10.1039/C3NR00970J
12. D. A. Pichugina, N. A. Nikitina, and N. E. Kuzmenko, J. Phys. Chem. C **124**, 3080 (2020). https://doi.org/10.1021/acs.jpcc.9b10286
13. V. Sudheeshkumar, K. O. Sulaiman, and R. W. J. Scott, Nanoscale Adv. **2**, 55 (2020). https://doi.org/10.1039/C9NA00549H
14. Y. Negishi, K. Munakata, W. Ohgake, et al., J. Phys. Chem. Lett. **3**, 2209 (2012). https://doi.org/10.1021/jz300892w
15. H. Yang, Y. Wang, J. Lei, et al., J. Am. Chem. Soc. **135**, 9568 (2013). https://doi.org/10.1021/ja402249s
16. Y. Negishi, T. Iwai, and M. Ide, Chem. Commun. **46**, 4713 (2010). https://doi.org/10.1039/C0CC01021A
17. E. B. Guidez, V. Mäkinen, H. Häkkinen, et al., J. Phys. Chem. C **116**, 20617 (2012). https://doi.org/10.1021/jp306885u
18. J. P. Perdew, M. Ernzerhof, and K. Burke, J. Chem. Phys. **105**, 9982 (1996). https://doi.org/10.1063/1.472933
19. D. N. Laikov, Chem. Phys. Lett. **416**, 116 (2005). https://doi.org/10.1016/j.cplett.2005.09.046
20. D. N. Laikov and Yu. A. Ustynyuk, Russ. Chem. Bull., No. 3, 820 (2005).
21. C. Zeng, C. Liu, Y. Chen, et al., J. Am. Chem. Soc. **136**, 11922 (2014). https://doi.org/10.1021/ja506802n